Biomaterials 41 (2015) 15–25

Contents lists available at ScienceDirect

Biomaterials

journal homepage: www.elsevier.com/locate/biomaterials

The effects of spheroid formation of adipose-derived stem cells in a microgravity bioreactor on stemness properties and therapeutic potential

Shichang Zhang [a], Ping Liu [a], Li Chen [b], Yingjie Wang [c], Zhengguo Wang [a], Bo Zhang [a, *]

[a] Department 4, Institute of Surgery Research, Daping Hospital, Third Military Medical University, State Key Lab of Trauma, Burns and Combined Injury, Chongqing 400042, China
[b] Department of Obstetrics and Gynecology, The First Affiliated Hospital of Nanjing Medical University, Nanjing, Jiangsu 210017, China
[c] Institute of Infectious Diseases, Southwest Hospital, Third Military Medical University, Chongqing 400038, China

ARTICLE INFO

Article history:
Received 18 August 2014
Accepted 7 November 2014
Available online 1 December 2014

Keywords:
Adipose-derived stem cells
Microgravity bioreactor
Stemness property
Therapeutic potential

ABSTRACT

Adipose-derived stem cells (ADSCs) represent a valuable source of stem cells for regenerative medicine, but the loss of their stemness during *in vitro* expansion remains a major roadblock. We employed a microgravity bioreactor (MB) to develop a method for biomaterial-free-mediated spheroid formation to maintain the stemness properties of ADSCs. ADSCs spontaneously formed three-dimensional spheroids in the MB. Compared with monolayer culture, the expression levels of E-cadherin and pluripotent markers were significantly upregulated in ADSC spheroids. Spheroid-derived ADSCs exhibited increased proliferative ability and colony-forming efficiency. By culturing the spheroid-derived ADSCs in an appropriate induction medium, we found that the multipotency differentiation capacities of ADSCs were significantly improved by spheroid culture in the MB. Furthermore, when ADSCs were administered to mice with carbon tetrachloride-induced acute liver failure, spheroid-derived ADSCs showed more effective potentials to rescue liver failure than ADSCs derived from constant monolayer culture. Our results suggest that spheroid formation of ADSCs in an MB enhances their stemness properties and increases their therapeutic potential. Therefore, spheroid culture in an MB can be an efficient method to maintain stemness properties, without the involvement of any biomaterials for clinical applications of *in vitro* cultured ADSCs.

1. Introduction

Stemness properties of mesenchymal stem cells (MSCs), which are capable of self-renewal and multi-lineage differentiation, endow them with great potential for tissue engineering and regenerative medicine [1]. Adipose-derived stem cells (ADSCs) represent an abundant source of MSCs that are easily accessible from subcutaneous adipose tissue via liposuction [2]. MSCs comprise only a small proportion of the bone marrow or adipose tissue, and they must be extensively expanded in culture to achieve the numbers required for any therapeutic strategy [3,4]. During *in vitro* expansion of common monolayer cultures, however, MSCs quickly lose their primitive stemness properties, such as replicative ability, colony-forming efficiency, and differentiation capacity [5,6]. Therefore, maintaining stemness properties has become a crucial issue for future clinical applications of *in vitro*-cultured ADSCs.

The stemness properties of MSCs are retained in the *in vivo* microenvironment, which comprises soluble growth factors, cell–cell interactions and cell–matrix interactions [7,8]. Accumulating evidence has suggested that the cellular microenvironment plays an important role in determining stemness properties [9,10]. Compared with conventional monolayer cultures, three-dimensional (3D) culture methods offer a cellular niche that is more similar to the *in vivo* microenvironment [11]. Several 3D cell culture methods, including the use of hydrogels, porous scaffolds or polymers, as well as cellular aggregates, have been developed to maintain the stemness properties of stem cells [12–14]. Among these methods, spheroid culture is a typical scaffold-free 3D cell culture system that takes advantage of the natural self-assembly tendency of numerous cell types [15]. Spheroid formation enables

* Corresponding author. Tel./fax: +86 23 68757443.
E-mail address: zhangbo67184@163.com (B. Zhang).

http://dx.doi.org/10.1016/j.biomaterials.2014.11.019
0142-9612/

cells to assemble and interact under native forces and allows them to generate their own extracellular matrix [16]. When cells contact, interact and communicate with other cells rather than with artificial scaffolds, the cell culture more closely replicates the *in vivo* environment [11]. Previous studies have demonstrated that spheroid formation of MSCs cultured on chitosan films or using hanging drop facilitated their stemness maintenance [16,17]. Furthermore, a recent study demonstrated that differentiated cells were reprogrammed by and acquired stemness properties from spheroid culture [18]. Therefore, spheroid culture may be an efficient method to maintain the stemness properties of MSCs.

Spheroids can be generally obtained via three approaches: hanging drop, low-attachment culture conditions, and dynamic culture [19–21]. Although the two former methods are convenient for generating homogeneous aggregates and do not cause shear stress damage, these techniques are not suitable for high-activity and large-scale production of spheroids. Dynamic cultures involve spheroids that are grown in a spinner flask or a microgravity bioreactor (MB) [16,22]. In addition to the obvious advantages of large-scale and high-density cell culture in a dynamic culture system, the MB also offers the benefits of reduced shear stress and increased mass transfer compared with spinner flask [22]. Cell damage caused by mechanical agitation is reduced by gentle shear stress [16]. Increased mass transfer promotes the transport of nutrients and the removal of metabolites from spheroids growing in an MB [23]. Thus, these advantages of MB potentially increase cell viability of MSCs. Moreover, increasing evidence has demonstrated that MBs are useful in the scale-up of stem cells [24,25]. Our previous studies have shown that MBs promote spheroid formation and large-scale expansion of stem cells [23]. Therefore, spheroid culture of MSCs in MB has a promise to not only meet fully the requirements of large-scale production as well as high-activity and high-density cell culture for clinical application, but also preserve their stemness properties. However, it is unclear whether the stemness properties of MSCs can be maintained or improved by spheroid culture in MB.

In this study, we employed an MB to develop a straightforward and effective method of biomaterial-free-mediated spheroid formation to improve the stemness properties of ADSCs for clinical application. The stemness properties of spheroid-derived ADSCs, including proliferative ability, pluripotent maker expression, colony-forming efficiency, and multipotency differentiation capacity, were investigated. We further examined the therapeutic potential of spheroid-derived ADSCs for carbon tetrachloride (CCl_4)-induced acute liver failure (ALF) in non-obese diabetic severe combined immunodeficient (NOD-SCID) mice. Possible mechanisms for the improvement of stemness properties are discussed based on spheroid formation of ADSCs in the MB.

2. Materials and methods

2.1. Isolation and culture of ADSCs

Subcutaneous adipose tissue was obtained from patients undergoing elective surgical procedures at the Department of Plastic Surgery. This study was approved by the Research Ethics Committee of the Daping Hospital and Third Military Medical University, and all participants provided informed written consent. ADSCs were isolated as described previously [26]. Freshly isolated cells were resuspended in Dulbecco's modified Eagle's medium (DMEM)/F12 (Gibco, Gaithersburg, MD) supplemented with 10% fetal bovine serum (FBS, Gibco) and 1% penicillin–streptomycin (Invitrogen, Carlsbad, CA). The cell suspensions were seeded into tissue culture flasks or MBs (Synthecon, Inc., Houston, TX) at a density of 10^6 cells/ml and incubated at 37 °C in humidified atmosphere with 5% CO_2. The MB was set to rotate at a speed of 25 rpm. Every 2–3 days, 80% of the culture medium was replaced with fresh medium. After 5 days of culture, ADSC spheroids aggregated in the MB were dissociated with trypsin/ethylenediaminetetraacetate (EDTA) solution (Gibco) and then transferred to a tissue culture flask for further experiments (spheroid-derived ADSCs). We used ADSCs that were continuously cultured in tissue culture flasks as the control (monolayer ADSCs).

2.2. Characteristics of ADSC spheroids

To calculate the size distribution of spheroids, spheroid suspensions were taken from the MB on days 1, 3 and 5. Images of spheroids were photographed using digital microscopy. The diameters of the spheroids were measured using Image Pro software (Media Cybernetics, Silver Spring, MD). For the apoptosis assay, spheroids were stained using a propidium iodide (PI, Sigma–Aldrich, St Louis, MO)/4,6-diamidino-2-phenylindole (DAPI, Sigma–Aldrich) apoptosis detection kit according to the manufacturer's instructions. The expression levels of stemness marker genes and E-cadherin in ADSC spheroids were analyzed by quantitative reverse transcription-polymerase chain reaction (RT-PCR) or immunofluorescence staining.

2.3. Morphology and proliferation viability of spheroid-derived ADSCs

After 5 days of culture, the spheroids were removed from the MB and placed directly into tissue culture flasks for culture. Cell morphology was observed using a phase-contrast microscopy. To investigate the proliferation viability of spheroid-derived ADSCs, spheroids in the MB were dissociated by trypsin/EDTA and then cultured at a density of 5×10^4 cells/ml under the same monolayer culture conditions as described above. Cells were lifted with trypsin/EDTA and then counted using a hemocytometer at various times during the 7-day period.

2.4. Colony-forming unit-fibroblast (CFU-F) assay

The CFU-F assay was performed using modified techniques as described previously [17]. ADSCs derived from monolayer and spheroids were cultured in culture medium at a density of 1000 cells per-100 mm dish. The medium was changed every 3 days. After 14 days of culture, the cells were fixed with 4% paraformaldehyde and stained with 3% crystal violet solution (Sigma–Aldrich). The number of colonies (diameter $\geq$ 2 mm) was counted.

2.5. In vitro multipotency differentiation assay

The spheroids were collected at 5 days, dissociated into single cells, and induced with different media for differentiation of the three germ layers. Adipogenic, osteogenic and chondrogenic differentiation of ADSCs derived from spheroids or monolayer cultures were performed as described previously [27]. After 4 weeks of induction, the adipogenic-specific genes peroxisome proliferator-activated receptor-γ (PPAR-γ) and lipoprotein lipase (LPL), the osteogenic-specific genes osteocalcin and osteopontin, and the chondrogenic-specific genes collagen II and aggrecan were detected by quantitative RT-PCR as described below. The cells were stained using the Oil red O procedure, Alizarin red or Alcian blue solution to further observe the presence of neutral lipid vacuoles in adipocytes, calcium deposition in osteocytes or collagen II in chondrocytes, respectively.

Hepatogenic and neurogenic differentiation of spheroid or monolayer ADSCs were selected to test the representative transdifferentiation capacities of endodermal and ectodermal lineages. Hepatogenic and neurogenic differentiation were induced as described in a previous study [17]. After 21 days of culture, the expression levels of hepatogenic (albumin, CK-18 and CYP3A4) or neurogenic (β-III tubulin and nestin) markers were analyzed by quantitative RT-PCR and immunofluorescence.

2.6. Quantitative RT-PCR

Total RNA was extracted from ADSCs derived from spheroids and monolayer cultures using the RNeasy Mini Kit (Qiagen, Inc., Valencia, CA) according to the manufacturer's instructions. The total RNA concentration was determined by optical density at 260 nm using a spectrophotometer. After removing residual DNA with DNase I, equal amounts of RNA (1 μg) were added to a reverse transcriptase reaction mixture with oligo-dT primers (Invitrogen). The Power SYBR Green RT-PCR Kit (Applied Biosystems, Foster City, CA) was used to perform quantitative RT-PCR using the Bio-Rad CFX96 Real-Time system (Bio-Rad Laboratories, Inc., Hercules, CA). The expression level was analyzed and normalized to GAPDH in the cDNA samples. The fold change of gene expression was calculated using the 2-ΔΔCT method. Primer sequences are provided in Table S1.

2.7. Immunofluorescence

Spheroids were taken from the MB after 5 days and seeded directly onto slides for 2 h of culture. Spheroids or cells on slides were fixed in 4% paraformaldehyde and washed three times with PBS, and they were then immersed in PBS containing 0.1% Triton X-100 (Sigma–Aldrich) and 1% normal serum for 30 min at room temperature. Samples were then incubated overnight at 4 °C with the following primary antibodies: rabbit anti-E-cadherin and goat anti-Oct4 (1:200, Santa Cruz Biotech, Inc., Santa Cruz, CA), rabbit anti-Nanog (1:400, Abcam, Cambridge, UK), goat anti-Sox2 (1:300, Invitrogen), rabbit anti-Rex-1 (1:400, Invitrogen), rabbit anti-ALB (1:500, Bethyl Laboratories, Montgomery, TX), rabbit anti-CK18 (1:200, Invitrogen), goat anti-CYP3A4 (1:200, Invitrogen), rabbit anti-β-III tubulin (1:400, Invitrogen), goat anti-nestin (1:400, Invitrogen). After incubation with primary antibodies, cells were washed with PBS and then incubated with FITC-conjugated goat anti-rabbit IgG or Cy5-conjugated donkey anti-goat IgG (1:400, Invitrogen) for 1 h at room temperature. Nuclear DNA was dyed with DAPI. Images were captured using the Leica confocal microscopy system.

2.8. Animal model and cell transplantation

NOD-SCID mice were purchased from the Laboratory Animal Center, Third Military Medical University. All of the procedures followed ethical guidelines and were approved by the Institutional Animal Care and Use Committee of Third Military Medical University. The animal model study and cell transplantation were performed as described in our previous report [28]. ALF was induced in male SCID mice by gavage of 10% CCl_4 (0.28 ml/kg body weight). CCl_4 induced liver injury causing apoptosis and necrosis of hepatocytes with 100% lethality at 72 h. Cell transplantation was performed under ethyl ether inhalation anesthesia at 24 h after administration of CCl_4. Direct intrasplenic injections were made after laparotomy. Three transplantation groups were designed: group A, control mice that received 100 μl of PBS (vehicle) injected into the spleen ($n = 10$); group B, mice that received 100 μl of monolayer ADSCs (4×10^7 cells/kg body weight) injected into the spleen ($n = 12$); and group C, mice that received 100 μl of spheroid-derived ADSCs (4×10^7 cells/kg body weight) injected into the spleen ($n = 12$). After transplantation, blood samples were collected at 2, 7, and 14 days. In addition, the entire livers were taken, fixed and prepared for further analysis from sacrificed mice.

2.9. Serum transaminase levels

Serum aspartate aminotransferase (AST) and alanine aminotransferase (ALT) levels in mouse blood were measured using an automated biochemical analyzer.

2.10. Histologic and immunohistochemical analyses

Livers were fixed in 4% formaldehyde for 24 h and embedded in paraffin. Liver sections (5 μm thick) were deparaffinized and fixed. For histology, sections were stained with hematoxylin–eosin (H&E, Sigma–Aldrich). For the terminal deoxynucleotidyl transferase (TdT)-mediated deoxyuridine triphosphate (dUTP)-biotin nick end labeling (TUNEL) procedure, an *in situ* apoptosis detection kit (Boehringer, Mannheim, Germany) was applied following the manufacturer's instructions. Non-specific reactions of the liver slides were blocked with 3% H_2O_2 for 10 min at room temperature. TdT and biotin-11-dUTP reactions were carried out for 1 h at 37 °C. Removal of TdT from the procedure provided a negative control. Horseradish peroxidase–3,3 diaminobenzidine was used for the TUNEL procedure, and hematoxylin was used as a counter stain. Hepatocyte apoptosis was calculated as the ratio of the number of TUNEL-positive cells to the total number of hepatocytes in each slide.

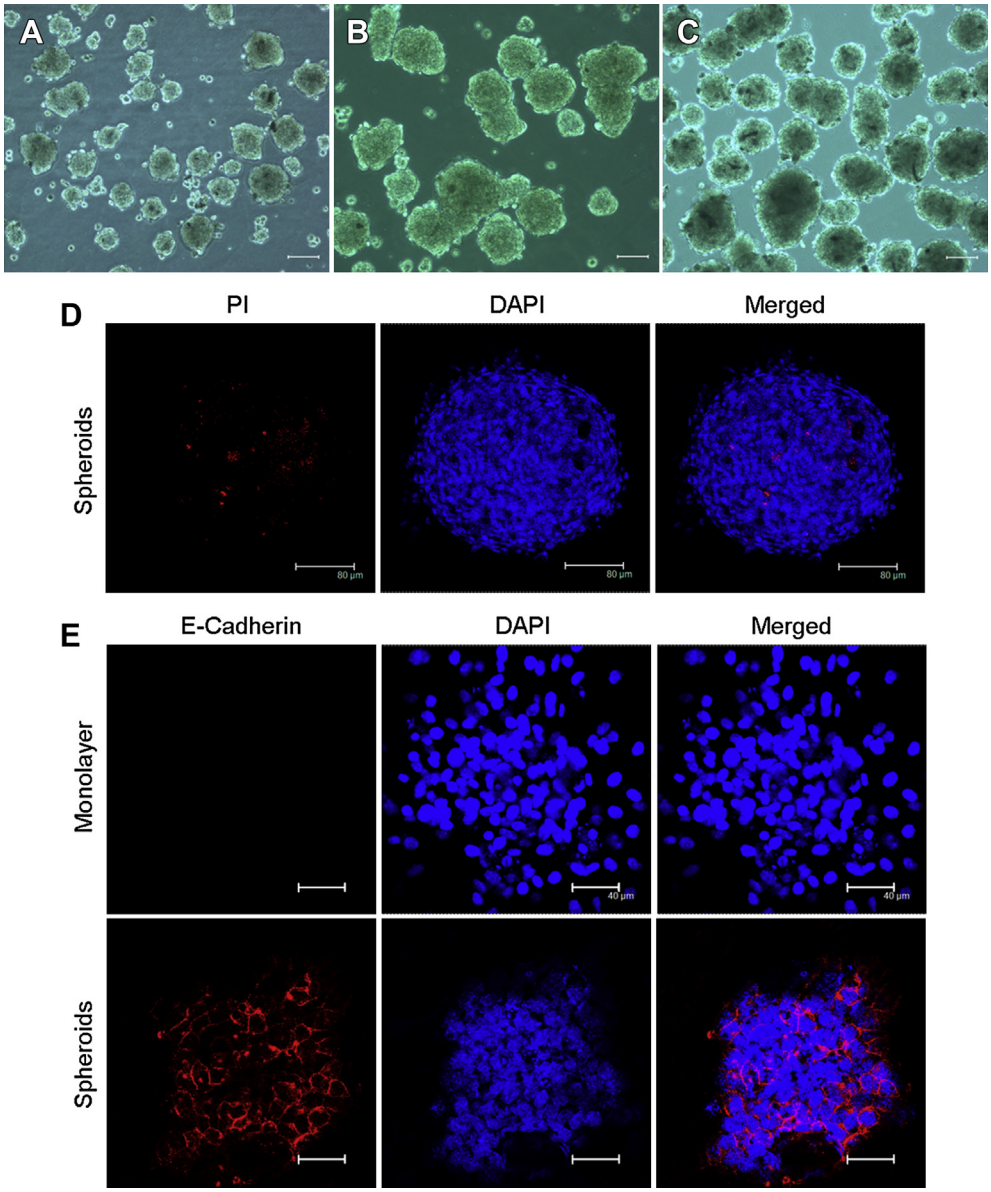

Fig. 1. Characteristics of ADSC spheroids in MB. A–C: Morphology of ADSC spheroids cultured in a microgravity bioreactor on day 1 (A), 3 (B), 5 (C). Scale bar: 100 μm. D: Confocal microscopic images of live/dead staining on day 5. Live cells within spheroids were stained with DAPI (blue), and dead cells were stained with PI (red). Scale bar: 80 μm. E: Immunofluorescence staining of ADSC spheroids for E-cadherin on day 5. Scale bar: 40 μm. ADSCs, adipose-derived stem cells; DAPI, 4,6-diamidino-2-phenylindole; MB, microgravity bioreactor; PI, propidium iodide. (For interpretation of the references to color in this figure legend, the reader is referred to the web version of this article.)

2.11. Statistical analysis

Statistical analyses were performed using PRISM 5.01 (GraphPad Software, Inc., San Diego, CA). Data are presented as the means ± SD of n determinations as indicated in the figure legends. Animal survival was analyzed by log-rank tests, and p values are as shown. All other data were analyzed using Student's t-test, where $p < 0.05$ was considered statistically significant. The Bonferroni correction was used for multiple comparisons.

3. Results

3.1. Spheroid formation of ADSCs cultured in the MB

When ADSCs were cultured in the MB, cells were aggregated into multicellular spheroids within 24 h. The size of spheroids increased gradually on days 1 and 5, and the number of suspended cells continued to decrease. The average spheroid diameters were 76.88 ± 25.55, 119.32 ± 52.93, and 123.47 ± 26.28 μm on days 1, 3, and 5, respectively (Fig. 1A–C). Spheroids were dissociated into single cells and reincubated in the MB, resulting in the generation of secondary spheroids. The viability of the cells within the spheroids was assessed by a live/dead assay after 5 days of MB culture. Cells that displayed necrosis in the center of the spheroid were stained red with PI, whereas the viable cells were stained blue with DAPI. Fig. 1D shows that most of the cells were viable within the spheroids from the MB culture, indicating the absence of necrotic centers. Moreover, immunofluorescence staining revealed a robust meshwork of E-cadherin inherent with its cell–cell contact in ADSC spheroids (Fig. 1E). By contrast, E-cadherin immunostaining of monolayer ADSCs was not positive.

3.2. The expression of pluripotent markers in ADSC spheroids

Oct4, Nanog, Sox-2 and Rex-1 are core transcription factors for embryonic stem cells, and they are important for maintaining the

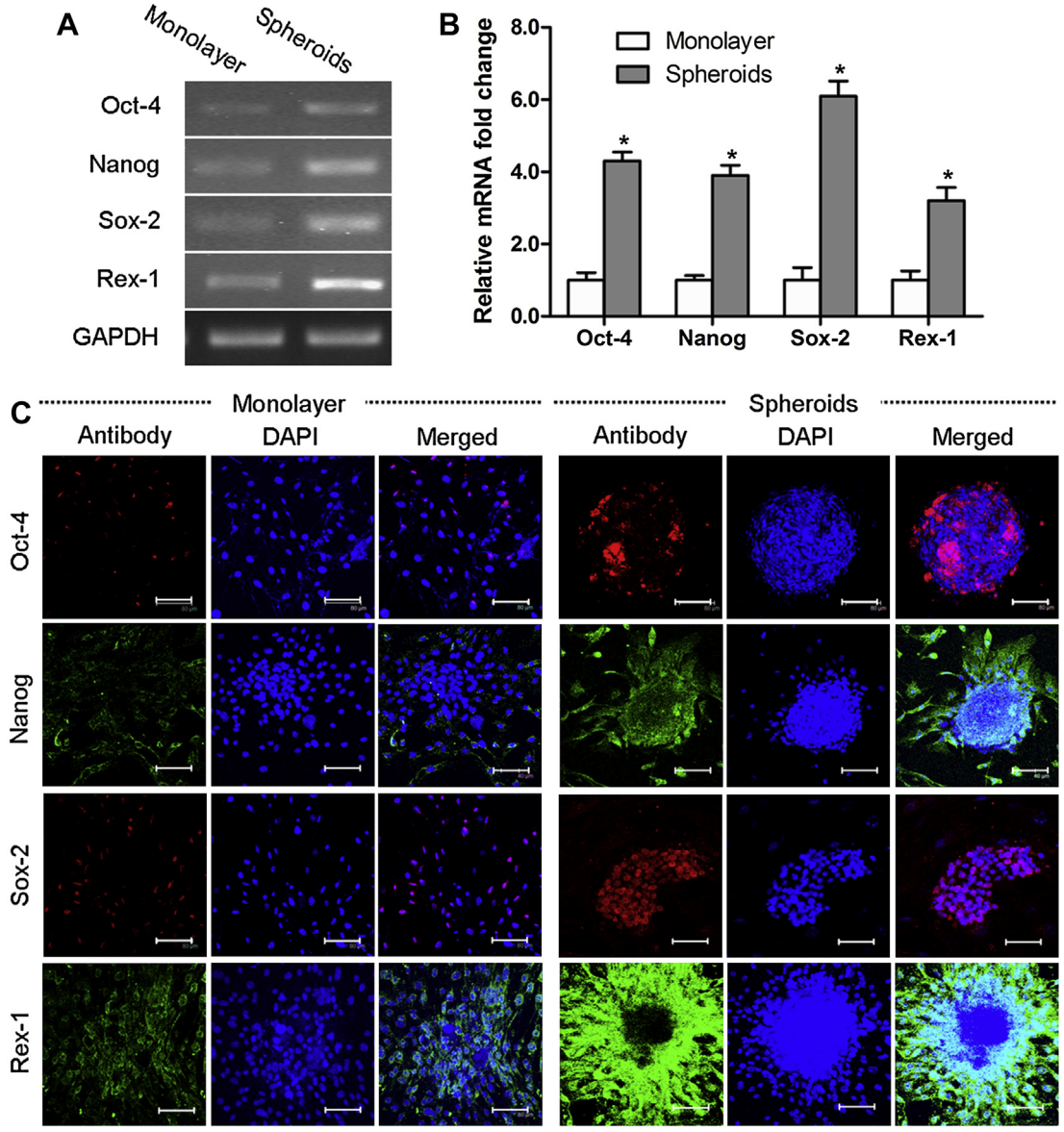

Fig. 2. Expression of pluripotent markers in ADSC spheroids and monolayer ADSCs on day 5. A: The genes Oct4, Nanog, Sox-2 and Rex-1 were analyzed by RT-PCR. B: The relative levels of these genes were assessed via quantitative RT-PCR. The results are expressed as the means ± SD of six experiments. $^{*}p < 0.05$ *vs.* monolayer ADSCs. C: Immunofluorescence staining for these pluripotent markers was performed on the day-5 spheroids cultured on chamber slides for 2 h. Scale bar: 80 μm. PCR, polymerase chain reaction. RT-PCR, reverse transcription-polymerase chain reaction.

pluripotency and self-renewal capacities of stem cells. The expression of the pluripotent markers Oct4, Nanog, Sox-2 and Rex-1 was analyzed by RT-PCR and immunofluorescence. RT-PCR analysis showed that Oct4, Nanog, Sox-2 and Rex-1 were upregulated in ADSC spheroids compared with monolayer ADSCs (Fig. 2A). Quantitative RT-PCR results revealed that ADSCs within spheroids exhibited significantly greater expression levels of Oct4, Nanog, Sox-2 and Rex-1 with 4.3 ± 0.3-fold, 3.9 ± 0.3-fold, 6.2 ± 0.4-fold, and 3.2 ± 0.4-fold increases, respectively, compared with monolayer ADSCs (Fig. 2B). We used immunofluorescence to further confirm that the protein levels of these genes were higher in spheroids than in monolayer ADSCs (Fig. 2C). These data demonstrate that spheroid formation of ADSCs in the MB promoted the expression of pluripotent markers, and this may facilitate the maintenance of the stemness properties of stem cells.

3.3. Proliferative ability of spheroid-derived ADSCs

To observe the difference in cell morphology, spheroids were directly cultured in tissue culture flasks. A large number of cells had grown around the spheroids after 1 day of culture. Microscopic inspection revealed that spheroid-derived ADSCs were heterogeneous in appearance, exhibiting round, spindle, and triangle shapes. Compared with monolayer ADSCs (Fig. 3A), a higher number of small cells that were round and bright were observed among the spheroid-derived ADSCs (Fig. 3B, C). We found that the round small cells grown in adherent culture spontaneously formed cell clusters (Fig. 3D). To evaluate the proliferation potential of cells within the spheroids, ADSC spheroids were dissociated and seeded back to a monolayer culture. Compared with monolayer ADSCs, spheroid-derived ADSCs exhibited significantly higher levels of proliferative ability at later time points (Fig. 3E). In addition, the

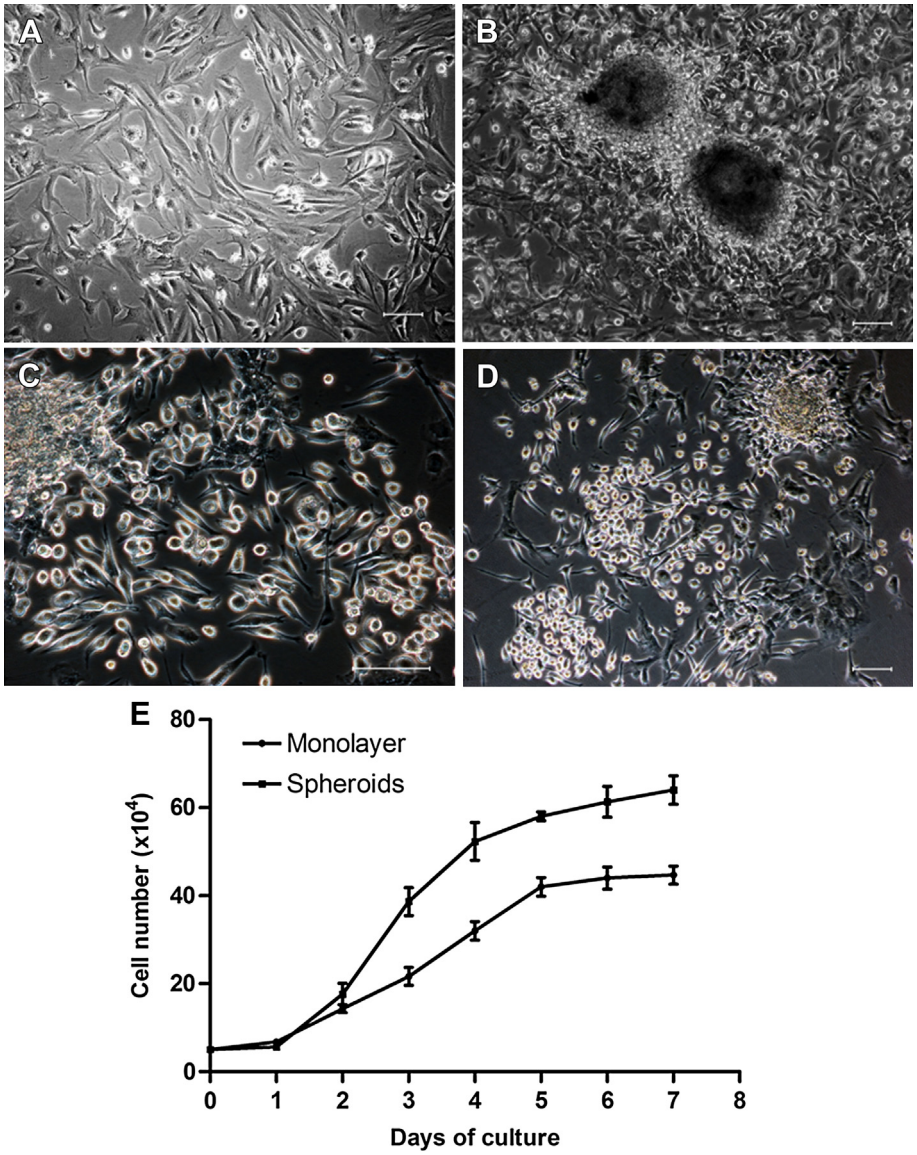

Fig. 3. Cell morphology and proliferative ability of ADSCs derived from spheroid and monolayer cultures. A–D: Phase-contrast images of ADSCs derived from monolayer (A) and spheroid (B–D) cultures. Scale bar: 100 μm. ADSC spheroids were directly cultured in tissue culture flasks. A large number of cells had grown around the spheroids after 1 day of culture. Spheroid-derived ADSCs exhibited various cell shapes, including round, spindle or triangle shapes (B). There were higher numbers of round and bright small cells among the spheroid-derived ADSCs (C). D: Spheroids in the MB were dissociated with trypsin/EDTA, and cultured under the same monolayer culture conditions. Small, round cells grown in adherent culture spontaneously formed cell clusters. E: Growth curves of ADSCs derived from monolayer and spheroid cultures at the initial seeding density of 5×10^4 cells/ml. The results are expressed as the means ± SD of six experiments. EDTA, ethylenediaminetetraacetate.

dissociated cells readily generated CFUs when plated at clonal densities (Fig. 4A, B). After 14 days of culture, more CFUs were generated by spheroid-derived ADSCs than by monolayer ADSCs (Fig. 4C–E).

3.4. Differentiation capabilities of spheroid-derived ADSCs

To investigate the effects of MB culture on the differentiation capabilities of ADSCs, spheroids were dissociated into single-cell suspensions and induced under the same conditions as monolayer ADSCs. Quantitative RT-PCR analysis of adipogenic markers showed that the expression levels of PPAR-γ and LPL were significantly increased in spheroid-derived ADSCs compared with monolayer ADSCs after adipogenic induction (Fig. 5A). Oil red O staining revealed higher numbers of positive cells in spheroid-derived ADSCs than in monolayer ADSCs (Fig. 5B, C). Moreover, spheroid-derived ADSCs exhibited higher expression levels of the osteogenic markers osteocalcin and osteopontin than monolayer ADSCs after the induction of osteogenesis (Fig. 5D). Increased calcium deposition in spheroid-derived ADSCs was detected by Alizarin red staining after osteogenic differentiation (Fig. 5E, F). Similarly, we also found that the expression levels of collagen II and aggrecan were significantly upregulated in spheroid-derived ADSCs compared with monolayer ADSCs after chondrogenic induction (Fig. 5G–I). These results demonstrate that the differentiation capabilities along the mesenchymal lineages of ADSCs were improved by spheroid formation in the MB.

Hepatogenic and neurogenic differentiation of MSCs represented the transdifferentiation capacities to the endoderm and ectoderm lineages. The results of quantitative RT-PCR revealed significantly increased transcription of ALB, CK-18, CYP3A4 (Fig. 6A) and β-III tubulin (Fig. 7A) in spheroid-derived ADSCs than in monolayer ADSCs after hepatogenic or neurogenic induction. Immunofluorescence images of these hepatogenic and neurogenic markers further confirmed that the protein expression levels of ALB, CK-18, CYP3A4 (Fig. 6B–D) and β-III tubulin (Fig. 7B) were higher in spheroid-derived ADSCs than in monolayer ADSCs after hepatogenic and neurogenic differentiation. However, there was no difference in the expression of nestin between spheroid-derived ADSCs and monolayer ADSCs after neurogenic induction (Fig. 7A, B). These data indicate that the transdifferentiation capabilities of ADSCs were enhanced by spheroid formation in the MB.

3.5. In vivo therapeutic potential of spheroid-derived ADSCs for ALF

To compare the therapeutic potential of spheroid-derived ADSCs with monolayer ADSCs for ALF, 4×10^7 ADSCs/kg body weight was intrasplenically transplanted under identical conditions after administration of CCl_4. All of the animals in the vehicle group died between 24 and 72 h after PBS treatment. At the 28-day endpoint, 75% of animals treated with spheroid-derived ADSCs were alive, whereas only 58% of animals treated with monolayer ADSCs survived. A significant survival benefit was observed for both spheroid-derived ADSC and monolayer ADSC groups compared with the vehicle group ($p < 0.05$), and there were also significant differences between the two ADSC groups ($p < 0.05$) (Fig. 8A). Liver serologies, including AST and ALT, were improved in animals treated with spheroid-derived ADSCs or monolayer ADSCs.

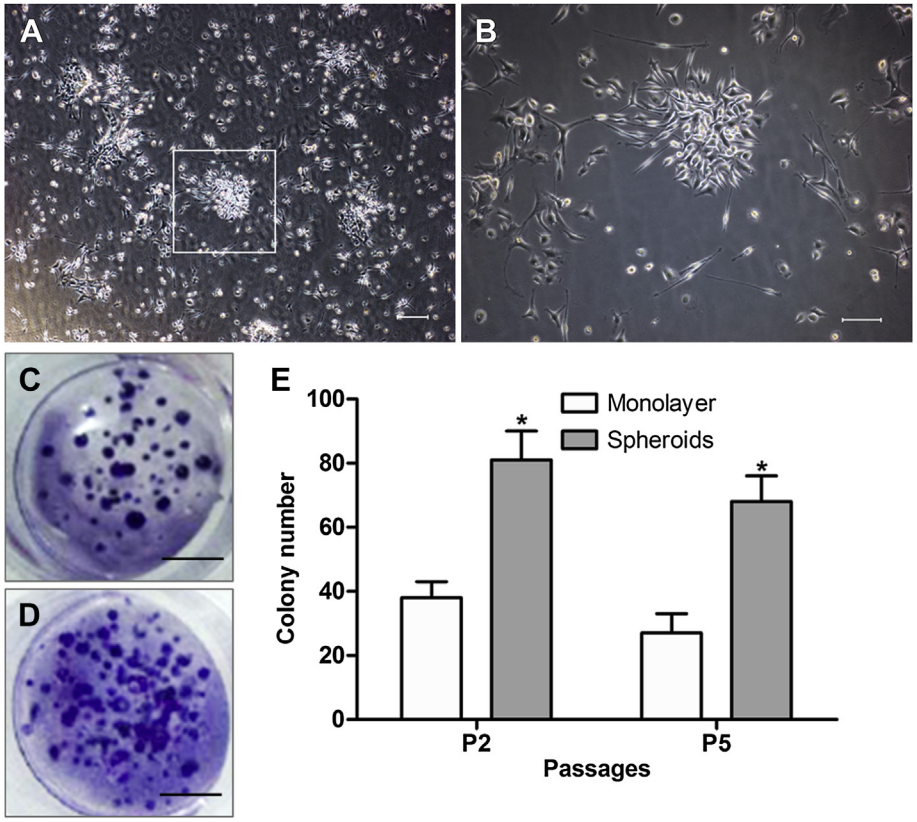

Fig. 4. Colony-forming efficiency of spheroid-derived ADSCs. CFU-F assays of ADSCs plated at 1000 cells/dish and incubated for 14 days. A, B: Phase-contrast images of CFU-F for spheroid-derived ADSCs. A: Scale bar: 200 μm. B: Scale bar: 100 μm. C, D: Crystal violet staining of CFU-F from monolayer ADSCs (C) and spheroid-derived ADSCs (D). Scale bar: 10 mm. E: The number of CFUs from spheroid-derived cells was significantly greater than the number of CFUs from monolayer ADSCs. The results are expressed as the means ± SD of six experiments. $^*p < 0.05$ *vs.* monolayer ADSCs. CFU-F, colony-forming unit-fibroblast.

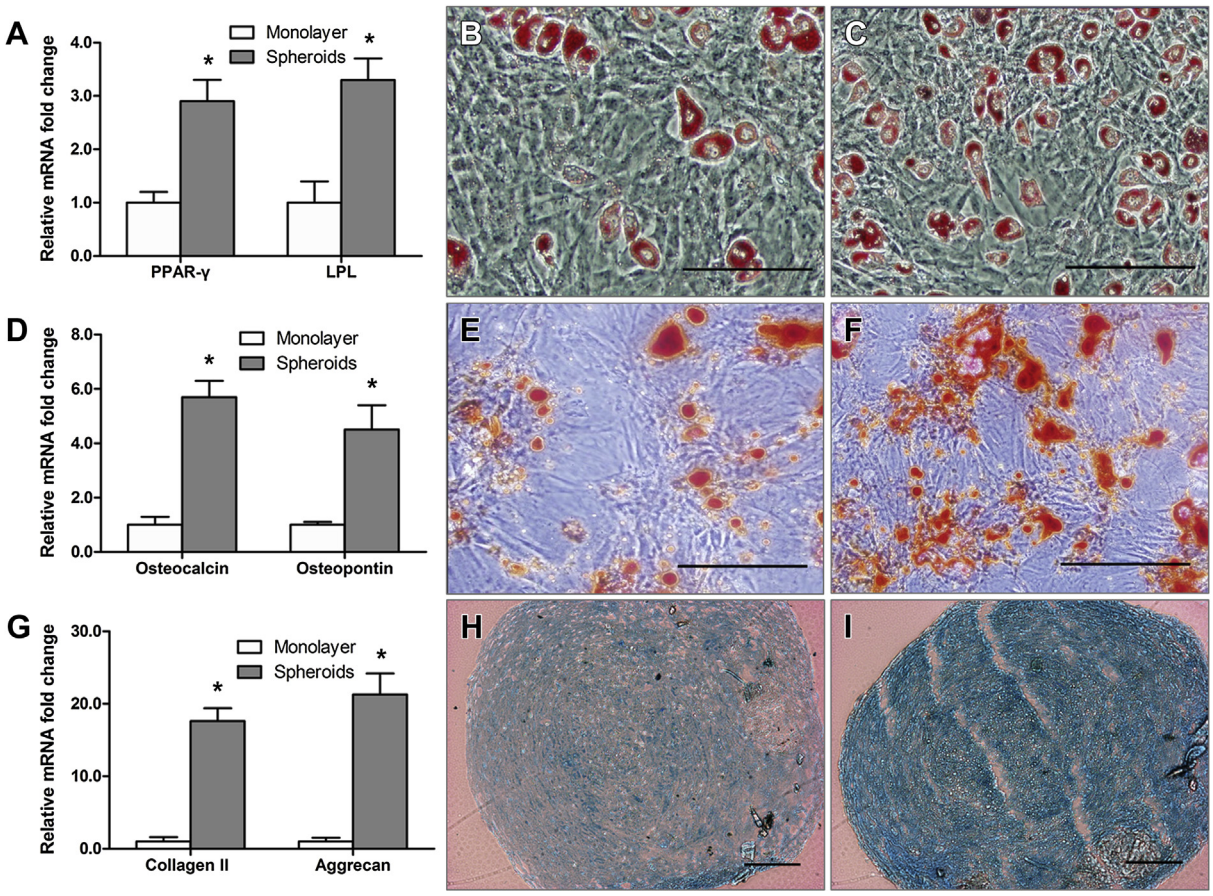

Fig. 5. Differentiation capabilities along the mesenchymal lineages of monolayer ADSCs and spheroid-derived ADSCs under the respective induction conditions for 28 days. A: Quantitative RT-PCR analysis of adipogenic marker gene expression levels. B, C: Staining of adipogenic monolayer ADSCs (B) and spheroid-derived ADSCs (C) with Oil red O. Scale bar: 100 μm. D: Quantitative RT-PCR analysis of osteogenic marker gene expression levels. E, F: Staining of osteogenic monolayer ADSCs (E) and spheroid-derived ADSCs (F) with Alizarin red. Scale bar: 100 μm. G: Quantitative RT-PCR analysis of chondrogenic marker gene expression levels. H, I: Staining of chondrogenic monolayer ADSCs (H) and spheroid-derived ADSCs (I) with Alcian blue. Scale bar: 100 μm. A, D, G: The results are expressed as the means ± SD of six experiments. $^{*}p < 0.05$ *vs.* monolayer ADSCs.

The improvement induced by spheroid-derived ADSCs was superior to that of monolayer ADSCs beginning at 2 days after transplantation (Fig. 8B, C). In addition, histological analysis of liver tissues revealed massive necrosis and hepatic lobule damage in pre-transplantation (Fig. 8D) and vehicle-treated mice (Fig. 8E). Cell necrosis was suppressed in the animals treated with monolayer ADSCs (Fig. 8F) or spheroid-derived ADSCs (Fig. 8G) beginning on day 14 after transplantation.

TUNEL staining was used to evaluate hepatocyte apoptosis in the liver sections. Widespread hepatocyte apoptosis was observed in the vehicle group (Fig. 9A), but the level of apoptosis decreased on days 2 and 7 after cell transplantation in the monolayer ADSC (Fig. 9B, D) and spheroid-derived ADSC (Fig. 9C, E) groups. Quantification of TUNEL-positive hepatocyte nuclei in animals treated with spheroid-derived ADSCs or monolayer ADSCs showed significant differences compared with vehicle-treated animals. The number of apoptotic cells was lower in animals treated with spheroid-derived ADSCs than in those treated with monolayer ADSCs at 2 days and 7 days post-transplantation (Fig. 9F).

4. Discussion

The stemness properties of stem cells may govern their therapeutic potentials in clinical applications. Maintaining the stemness properties of ADSCs remains a challenging issue during *in vitro* expansion [9]. Although previous studies have indicated that spheroid formation of ADSCs on several biomaterials or using hanging drop retain their stemness properties, these methods of spheroid culture do not fully meet the requirements of large-scale expansion for clinical application [17,20]. Our previous study and other studies have demonstrated that the MB culture system exhibits unique advantages in spheroid formation and large-scale production of stem cells [23,24]. However, the effects of spheroid formation of ADSCs in MB on their stemness properties have not been reported. In the present study, we demonstrated that ADSCs can form compact cellular spheroids and remain viable when cultured in the MB. This finding was consistent with a previous study [16], which exclusively investigated the effects of MB culture on the immunophenotype, osteogenic and adipogenic differentiation, and interleukin-24 (IL-24) secretion of MSCs. Our study focused on the changes in their stemness properties after spheroid formation of ADSCs in the MB. We identified their stemness properties based on various aspects, including pluripotent markers, proliferative ability, colony-forming efficiency, and differentiation or transdifferentiation capacities. Furthermore, the therapeutic potential of spheroid-derived ADSCs was examined in a mouse model of ALF. Our results suggest that spheroid formation in the MB enhanced the stemness properties and increased the therapeutic potential of ADSCs, without the involvement of any biomaterials, exogenous genes, or proteins.

Several core transcription factors, such as Oct4, Nanog, Sox-2 and Rex-1, are required to maintain the stemness properties of

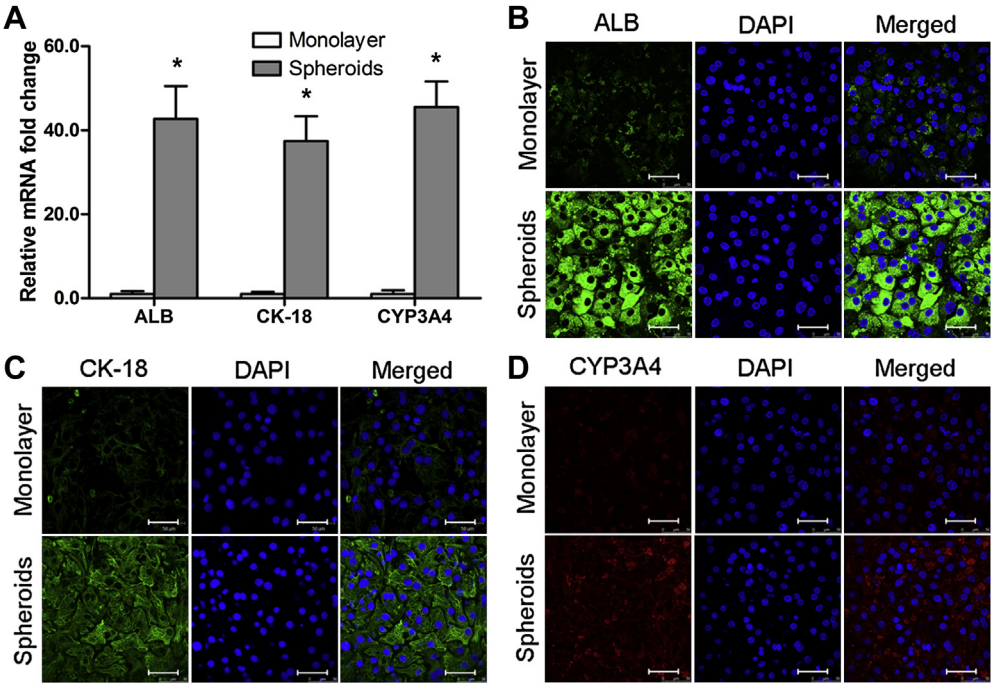

Fig. 6. Expression of hepatogenic transdifferentiation markers in monolayer ADSCs and spheroid-derived ADSCs using the same induction medium for 21 days. A: Quantitative RT-PCR analysis of hepatogenic markers. The results are expressed as the means ± SD of six experiments. *$p < 0.05$ *vs.* monolayer ADSCs. B–D: Immunofluorescence images of ALB (B), CK-18 (C) and CYP3A4 (D) representing hepatogenic induction. Scale bar: 50 μm. ALB, albumin; CK-18, cytokeratin-18; CYP3A4, cytochrome P450 3A4.

embryonic stem cells [29]. These pluripotent markers are also present in adult stem cells [5,30], including ADSCs, and they can alter the self-renewal and differentiation capabilities of these cells. However, the expression of the pluripotent genes declined with *in vitro* passaging of ADSCs, and this may result in the impairment of their therapeutic potential [6]. It has been reported that expression of these genes in MSCs was upregulated by spheroid formation in microwells or on biomaterial surfaces [17,31]. The effects of spheroid culture in the MB on these pluripotent markers of MSCs remain unclear. In the present study, the expression of the pluripotent markers Oct4, Nanog, Sox-2 and Rex-1 was significantly enhanced by spheroid formation of ADSCs in the MB compared with monolayer ADSCs. The expression levels of these genes can strongly influence proliferative activity [32]. We further found that spheroid-derived ADSCs possessed a higher proliferative rate and a higher colony-forming efficiency, suggesting that spheroid formation in the MB facilitates self-renewal in ADSCs.

The increased expression of the pluripotent markers found in our study may indicate better plasticity of ADSCs derived from spheroids. Our findings showed that spheroid formation of ADSCs in the MB improved their efficiency of differentiation along the mesoderm lineages. The enhanced osteogenic and adipogenic differentiation is consistent with data from Frith et al. [16], who used an MB as a dynamic MSC spheroid model. The upregulated pluripotent genes of MSCs alter cell fate and allow transdifferentiation [33]. Our data further demonstrated that spheroid-derived ADSCs exhibited significantly enhanced hepatogenic and neurogenic transdifferentiation capabilities compared with monolayer ADSCs when cultured in appropriate induction medium. Therefore, these results suggest that the multipotent differentiation of ADSCs was strengthened by spheroid formation in the MB, which may facilitate de-differentiation into a more primitive state.

The enhanced stemness properties of spheroid-derived ADSCs may exert beneficial effects on their therapeutic potential. Several recent reports have demonstrated that spheroid formation of

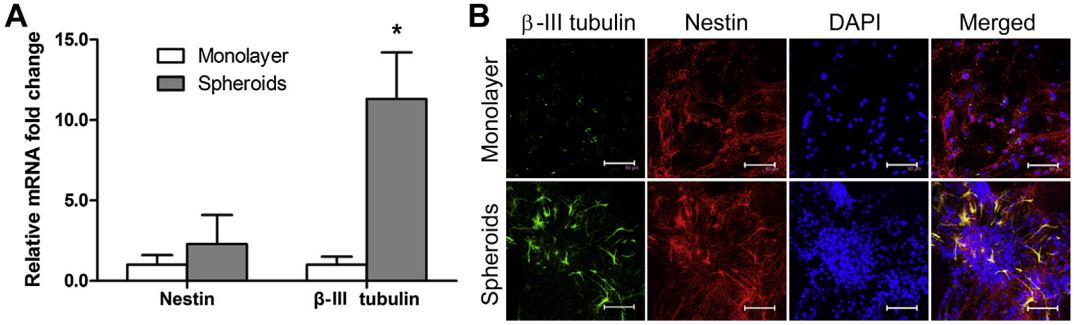

Fig. 7. Expression of neurogenic transdifferentiation markers in monolayer ADSCs and spheroid-derived ADSCs using the same induction medium for 21 days. A: Quantitative RT-PCR analysis of neurogenic markers. The results are expressed as the means ± SD of six experiments. *$p < 0.05$ *vs.* monolayer ADSCs. B: Immunofluorescence images of nestin and β-III tubulin, representing neurogenic induction. Scale bar: 80 μm.

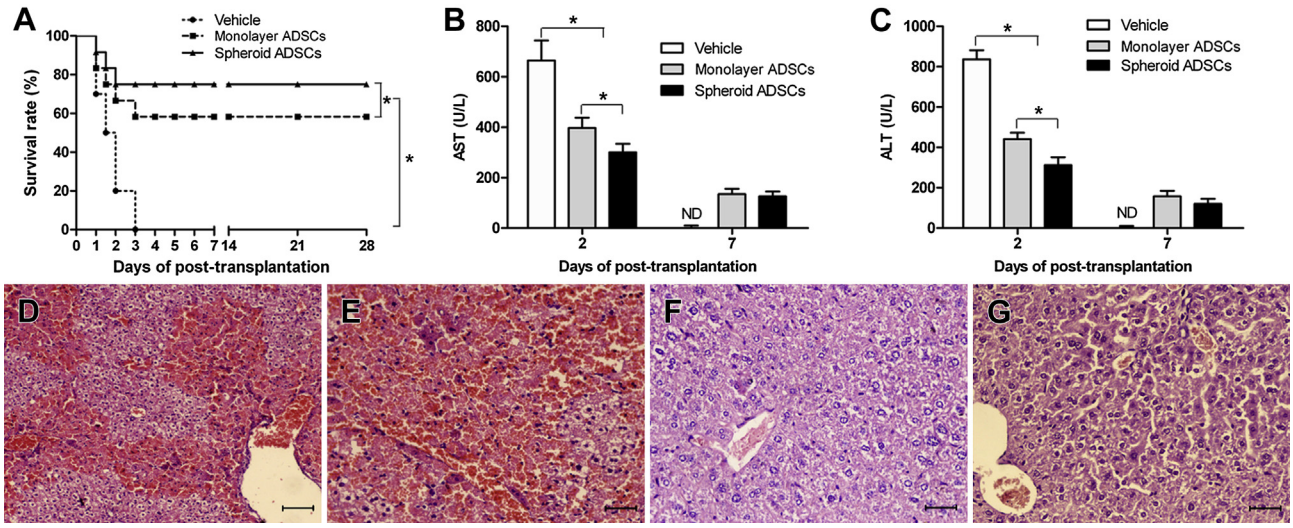

Fig. 8. Therapeutic potential of spheroid-derived ADSCs for ALF in a mouse model induced with 10% CCl_4. A: Kaplan–Meier survival analysis of CCl_4-induced NOD-SCID mice. $^*p < 0.05$. B, C: AST and ALT enzyme release levels in peripheral blood samples collected at 2 and 7 days after transplantation. $^*p < 0.05$. D–G: Histopathological recovery from CCl_4-induced ALF after transplantation with ADSCs. Hematoxylin and eosin staining of liver tissues revealed massive necrosis and hepatic lobule damage in pre-transplantation (D) and vehicle-treated mice (E). Cell necrosis was suppressed in the animals treated with monolayer ADSCs (F) or spheroid-derived ADSCs (G) beginning on day 14 after transplantation. Scale bar: 50 μm. ALF, acute liver failure; ALT, aspartate aminotransferase; AST, alanine aminotransferase; CCl_4, carbon tetrachloride; NOD-SCID, non-obese diabetic severe combined immunodeficient.

ADSCs on chitosan films increased their stemness properties and accelerated wound closure in a murine model of impaired cutaneous wounds [17,20,34]. We observed that spheroid-derived ADSCs showed more effective potential in rescuing liver failure than ADSCs derived from constant monolayer culture in a murine model of CCl_4-induced ALF, suggesting that the therapeutic potential of ADSCs was improved along with their enhanced stemness properties after spheroid culture in the MB. TUNEL staining further revealed that the inhibited hepatocyte apoptosis of ADSCs was significantly enhanced by spheroid culture in the MB. The latter finding was consistent with other reports showing that spheroid formation of MSCs could be used to enhance certain therapeutic activities, such as anti-inflammation, anti-apoptosis, angiogenesis, and homing to injury sites [34–36]. It has been reported that spheroid formation of MSCs in an MB improved their anti-cancer potential by increasing the expression of IL-24 [16]. The present *in vivo* study showed that spheroid culture in the MB increased the therapeutic potential of ADSCs, and this increase may be attributed to enhancing their stemness properties.

Several studies have demonstrated that the increased therapeutic potential of spheroid-derived ADSCs is closely associated with enhanced stemness properties [12,33,34]. The possible

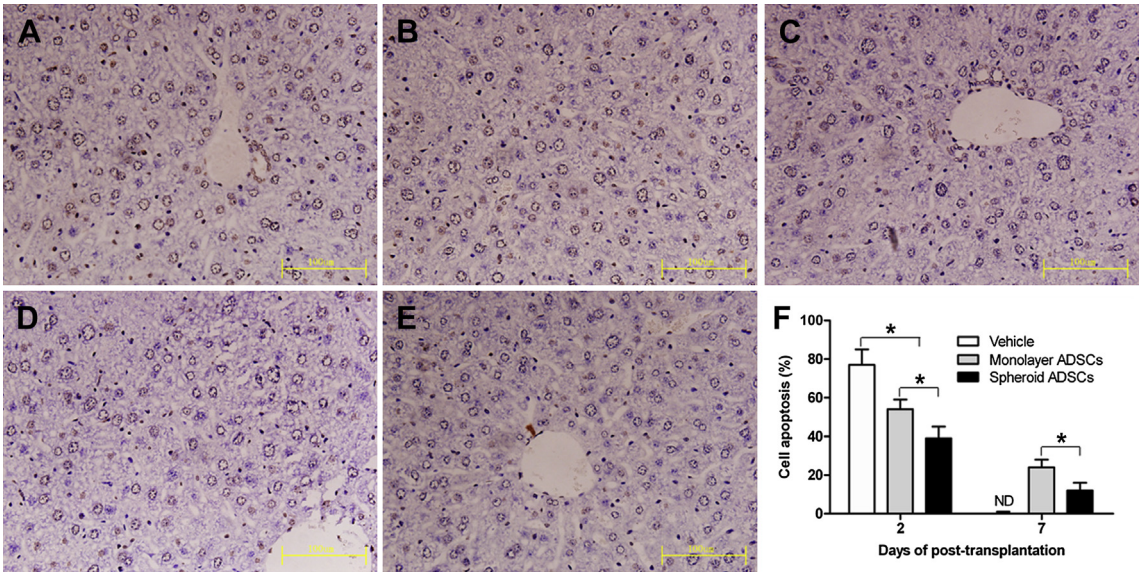

Fig. 9. Effect of spheroid-derived ADSCs on hepatocyte apoptosis in the livers of CCl_4-induced ALF mice. Liver sections were stained by TUNEL (brown nuclei, large for hepatocytes) and counterstained with hematoxylin (blue). A–E: Representative images from vehicle-treated (A), monolayer ADSC-treated (B, C) and spheroid-derived ADSC-treated (D, E) mice at day 2 (B, D) and day 7 (C, E). Scale bar: 100 μm. F: Quantification of TUNEL-positive hepatocytes by digital image analysis. The results are expressed as the means ± SD for 10 random fields per animal. $^*p < 0.05$. TUNEL, terminal deoxynucleotidyl transferase (TdT)-mediated deoxyuridine triphosphate (dUTP)-biotin nick end labeling. (For interpretation of the references to color in this figure legend, the reader is referred to the web version of this article.)

mechanisms for improving the survival of mice with acute liver failure by MSC transplantation may involve the ability of these cells to differentiate into hepatocyte-like cells, to reduce inflammation, and to enhance tissue repair at the site of injury by their paracrine or immunomodulatory capacities [37]. These mechanisms are likely independent, but not mutually exclusive. In many circumstances, these mechanisms potentially work in combination to promote the restoration of liver failure [38]. However, these actions of MSCs are based on the maintenance of their stemness properties [39,40]. The enhanced stemness properties of MSCs increase their proliferative ability and differentiation potential [41]. The increased proliferative ability of MSCs not only facilitates *in vitro* or *in vivo* expansion, but also improves cellular retention, integration and long-term survival after transplantation [12,17]. Increased cellular retention in the liver generates increased levels of paracrine or immunomodulatory factors to promote liver tissue regeneration [42]. Moreover, the maintenance of multipotency enables more MSCs to differentiate into hepatocyte-like cells and thus to compensate for impaired liver function [43]. Therefore, the enhanced stemness properties of spheroid-derived ADSCs results in their increased therapeutic potential. Further mechanistic studies are necessary in the future.

The molecular mechanisms that enhance the stemness properties of ADSC spheroids in MBs are intriguing but unclear. The stem cells' niche may determine their stemness properties [44]. Spheroid formation of stem cells might provide a microenvironment that facilitates stemness maintenance. First, inner hypoxia can occur in spheroids but not in monolayer culture, as reported by numerous studies demonstrating that hypoxic conditions help to maintain the pluripotency of stem cells [45]. Second, cell shape is a potent regulator of cell growth, physiology, embryonic development and stem cell differentiation, which potentially promotes cytoskeleton reorganization [46]. We observed that spheroid-derived ADSCs exhibited different morphologies from monolayer controls. Third, the extracellular matrix exerts extensive control over stem cell fate decisions through the actions of several classes of receptors [47], with integrins representing the most widely studied [48,49]. Spheroid formation may generate a distinct extracellular matrix and establish new cell–matrix interactions that can influence cell fate. In addition, stemness maintenance may be caused by the concentration gradients of oxygen, soluble factors and signaling factors in spheroids [50]. However, cell–cell interactions that regulate many biological processes such as cell shape, extracellular matrix, oxygen and nutrition gradients, and signal transduction, are mediated by direct cell contact or communication between cells [11]. Therefore, it is crucial that spheroid formation *in vitro* can establish the cell–cell contact required to reconstruct the microenvironment for improving the stemness properties of ADSCs.

Cell–cell contact is mainly mediated by cadherins. E-Cadherin is a key member of the cadherin family that is primarily responsible for tight junctions of cell–cell interactions. To the best of our knowledge, no study has reported E-cadherin expression in MSCs under monolayer culture conditions. In the current study, we also did not detect E-cadherin expression in monolayer ADSCs. However, our results showed that most of the ADSCs in spheroids expressed E-cadherin, suggesting the formation of tight junctions within ADSC spheroids. Similar to a previous study, the gene expression of E-cadherin in MSCs derived from umbilical cord blood was significantly increased by spheroid formation when the cells were cultured in suspension using a low-attachment dish [51]. Moreover, that previous study showed that antibody neutralization of the extracellular domain of E-cadherin inhibited spheroid formation of MSCs, indicating that E-cadherin plays a key role in the spheroid formation of MSCs. Activation of E-cadherin in association with cell–cell interaction during spheroid formation facilitated the increased proliferative and paracrine capacities of MSCs [51]. It has been reported that E-cadherin in ESCs plays an important role in maintaining stemness properties and is involved in restoring their pluripotency [52]. Upregulation of E-cadherin can improve the efficiency of fibroblast to iPS cell reprogramming by enhancing the mesenchymal-to-epithelial transition [53]. E-Cadherin may regulate pluripotency by ensuring that fully compacted cells have access to putative critical autocrine signals or by promoting the cell–cell exchange of signals, perhaps through gap junctions [54]. E-Cadherin has also been linked to pluripotency in human ESCs, likely because the promoter region of E-cadherin contains Oct3/4 binding sites [55]. Therefore, we believe that the mechanism of improving the stemness properties of ADSCs by spheroid formation in an MB is due to the upregulation of E-cadherin expression. Further investigation of the underlying mechanisms is warranted in the future.

5. Conclusions

Here, we report that stemness properties, including self-renewal and multipotency differentiation capacities, were enhanced by spheroid formation of ADSCs in an MB. We further demonstrate that the therapeutic potential of ADSCs was improved by spheroid culture in an MB. Moreover, an MB is a suitable tool for the large-scale preparation of spheroids and expansion of MSCs. Therefore, in the future, spheroid formation of ADSCs in an MB may be an efficient method to enhance their stemness properties for clinical applications of *in vitro*-cultured ADSCs without the involvement of any biomaterials, exogenous genes, or proteins.

Acknowledgments

This research was supported by funds from the National Program on Key Basic Research Project of China (2011CB964701), the National Natural Science Foundation of China (30800237) and the Foundation for Science and Technology Research Project of Chongqing (CSTC2012GGB1003). We gratefully acknowledge all of the members of the laboratory for sharing reagents and advice.

Appendix A. Supplementary data

Supplementary data related to this article can be found at http://dx.doi.org/10.1016/j.biomaterials.2014.11.019.

References

[1] Ma J, Both SK, Yang F, Cui FZ, Pan J, Meijer GJ, et al. Concise review: cell-based strategies in bone tissue engineering and regenerative medicine. Stem Cells Transl Med 2014;3:98–107.
[2] Cawthorn WP, Scheller EL, MacDougald OA. Adipose tissue stem cells: the great WAT hope. Trends Endocrinol Metab 2012;23:270–7.
[3] Fraser JK, Wulur I, Alfonso Z, Hedrick MH. Fat tissue: an underappreciated source of stem cells for biotechnology. Trends Biotechnol 2006;24:150–4.
[4] Gimble JM, Bunnell BA, Guilak F. Human adipose-derived cells: an update on the transition to clinical translation. Regen Med 2012;7:225–35.
[5] Baer PC, Griesche N, Luttmann W, Schubert R, Luttmann A, Geiger H. Human adipose-derived mesenchymal stem cells in vitro: evaluation of an optimal expansion medium preserving stemness. Cytotherapy 2010;12:96–106.
[6] Park E, Patel AN. Changes in the expression pattern of mesenchymal and pluripotent markers in human adipose-derived stem cells. Cell Biol Int 2010;34:979–84.
[7] Watt FM, Hogan BL. Out of Eden: stem cells and their niches. Science 2000;287:1427–30.
[8] Ramalho-Santos M, Yoon S, Matsuzaki Y, Mulligan RC, Melton DA. "Stemness": transcriptional profiling of embryonic and adult stem cells. Science 2002;298:597–600.
[9] Yan XZ, van den Beucken JJ, Both SK, Yang PS, Jansen JA, Yang F. Biomaterial strategies for stem cell maintenance during in vitro expansion. Tissue Eng Part B Rev 2014;20(4):340–54.
[10] Lu D, Luo C, Zhang C, Li Z, Long M. Differential regulation of morphology and stemness of mouse embryonic stem cells by substrate stiffness and topography. Biomaterials 2014;35:3945–55.
[11] Marx V. Cell culture: a better brew. Nature 2013;496:253–8.

[12] Emmert MY, Wolint P, Wickboldt N, Gemayel G, Weber B, Brokopp CE, et al. Human stem cell-based three-dimensional microtissues for advanced cardiac cell therapies. Biomaterials 2013;34:6339–54.
[13] Wei J, Han J, Zhao Y, Cui Y, Wang B, Xiao Z, et al. The importance of three-dimensional scaffold structure on stemness maintenance of mouse embryonic stem cells. Biomaterials 2014;35:7724–33.
[14] Rustad KC, Wong VW, Sorkin M, Glotzbach JP, Major MR, Rajadas J, et al. Enhancement of mesenchymal stem cell angiogenic capacity and stemness by a biomimetic hydrogel scaffold. Biomaterials 2012;33:80–90.
[15] Kapur SK, Wang X, Shang H, Yun S, Li X, Feng G, et al. Human adipose stem cells maintain proliferative, synthetic and multipotential properties when suspension cultured as self-assembling spheroids. Biofabrication 2012;4:025004.
[16] Frith JE, Thomson B, Genever PG. Dynamic three-dimensional culture methods enhance mesenchymal stem cell properties and increase therapeutic potential. Tissue Eng Part C Methods 2010;16:735–49.
[17] Cheng NC, Wang S, Young TH. The influence of spheroid formation of human adipose-derived stem cells on chitosan films on stemness and differentiation capabilities. Biomaterials 2012;33:1748–58.
[18] Su G, Zhao Y, Wei J, Han J, Chen L, Xiao Z, et al. The effect of forced growth of cells into 3D spheres using low attachment surfaces on the acquisition of stemness properties. Biomaterials 2013;34:3215–22.
[19] Spelke DP, Ortmann D, Khademhosseini A, Ferreira L, Karp JM. Methods for embryoid body formation: the microwell approach. Methods Mol Biol 2011;690:151–62.
[20] Huang GS, Dai LG, Yen BL, Hsu SH. Spheroid formation of mesenchymal stem cells on chitosan and chitosan-hyaluronan membranes. Biomaterials 2011;32:6929–45.
[21] Yeh HY, Liu BH, Hsu SH. The calcium-dependent regulation of spheroid formation and cardiomyogenic differentiation for MSCs on chitosan membranes. Biomaterials 2012;33:8943–54.
[22] Saleh FA, Frith JE, Lee JA, Genever PG. Three-dimensional in vitro culture techniques for mesenchymal stem cells. Methods Mol Biol 2012;916:31–45.
[23] Zhang S, Zhang Y, Chen L, Liu T, Li Y, Wang Y, et al. Efficient large-scale generation of functional hepatocytes from mouse embryonic stem cells grown in a rotating bioreactor with exogenous growth factors and hormones. Stem Cell Res Ther 2013;4:145.
[24] Fridley KM, Fernandez I, Li MT, Kettlewell RB, Roy K. Unique differentiation profile of mouse embryonic stem cells in rotary and stirred tank bioreactors. Tissue Eng Part A 2010;16:3285–98.
[25] Li S, Ma Z, Niu Z, Qian H, Xuan D, Hou R, et al. NASA-approved rotary bioreactor enhances proliferation and osteogenesis of human periodontal ligament stem cells. Stem Cells Dev 2009;18:1273–82.
[26] Shah FS, Wu X, Dietrich M, Rood J, Gimble JM. A non-enzymatic method for isolating human adipose tissue-derived stromal stem cells. Cytotherapy 2013;15:979–85.
[27] Zamperone A, Pietronave S, Merlin S, Colangelo D, Ranaldo G, Medico E, et al. Isolation and characterization of a spontaneously immortalized multipotent mesenchymal cell line derived from mouse subcutaneous adipose tissue. Stem Cells Dev 2013;22:2873–84.
[28] Zhang S, Chen L, Liu T, Zhang B, Xiang D, Wang Z, et al. Human umbilical cord matrix stem cells efficiently rescue acute liver failure through paracrine effects rather than hepatic differentiation. Tissue Eng Part A 2012;18:1352–64.
[29] Loh KM, Lim B. A precarious balance: pluripotency factors as lineage specifiers. Cell Stem Cell 2011;8:363–9.
[30] Riekstina U, Cakstina I, Parfejevs V, Hoogduijn M, Jankovskis G, Muiznieks I, et al. Embryonic stem cell marker expression pattern in human mesenchymal stem cells derived from bone marrow, adipose tissue, heart and dermis. Stem Cell Rev 2009;5:378–86.
[31] Baraniak PR, McDevitt TC. Scaffold-free culture of mesenchymal stem cell spheroids in suspension preserves multilineage potential. Cell Tissue Res 2012;347:701–11.
[32] Liu TM, Wu YN, Guo XM, Hui JH, Lee EH, Lim B. Effects of ectopic Nanog and Oct4 overexpression on mesenchymal stem cells. Stem Cells Dev 2009;18:1013–22.
[33] Yu J, Tu YK, Tang YB, Cheng NC. Stemness and transdifferentiation of adipose-derived stem cells using L-ascorbic acid 2-phosphate-induced cell sheet formation. Biomaterials 2014;35:3516–26.
[34] Cheng NC, Chen SY, Li JR, Young TH. Short-term spheroid formation enhances the regenerative capacity of adipose-derived stem cells by promoting stemness, angiogenesis, and chemotaxis. Stem Cells Transl Med 2013;2:584–94.
[35] Cho HJ, Lee HJ, Youn SW, Koh SJ, Won JY, Chung YJ, et al. Secondary sphere formation enhances the functionality of cardiac progenitor cells. Mol Ther 2012;20:1750–66.
[36] Laschke MW, Schank TE, Scheuer C, Kleer S, Schuler S, Metzger W, et al. Three-dimensional spheroids of adipose-derived mesenchymal stem cells are potent initiators of blood vessel formation in porous polyurethane scaffolds. Acta Biomater 2013;9:6876–84.
[37] Volarevic V, Nurkovic J, Arsenijevic N, Stojkovic M. Concise review: therapeutic potential of mesenchymal stem cells for the treatment of acute liver failure and cirrhosis. Stem Cells 2014;32(11):2818–23.
[38] Meier RP, Muller YD, Morel P, Gonelle-Gispert C, Buhler LH. Transplantation of mesenchymal stem cells for the treatment of liver diseases, is there enough evidence? Stem Cell Res 2013;11:1348–64.
[39] Saraswati S, Deskins DL, Holt GE, Young PP. Pyrvinium, a potent small molecule Wnt inhibitor, increases engraftment and inhibits lineage commitment of mesenchymal stem cells (MSCs). Wound Repair Regen 2012;20:185–93.
[40] Bongso A, Fong CY. The therapeutic potential, challenges and future clinical directions of stem cells from the Wharton's jelly of the human umbilical cord. Stem Cell Rev 2013;9:226–40.
[41] Trohatou O, Zagoura D, Bitsika V, Pappa KI, Antsaklis A, Anagnou NP, et al. Sox2 suppression by miR-21 governs human mesenchymal stem cell properties. Stem Cells Transl Med 2014;3:54–68.
[42] Russo FP, Parola M. Stem and progenitor cells in liver regeneration and repair. Cytotherapy 2011;13:135–44.
[43] Fausto N. Liver regeneration and repair: hepatocytes, progenitor cells, and stem cells. Hepatology 2004;39:1477–87.
[44] Moore KA, Lemischka IR. Stem cells and their niches. Science 2006;311:1880–5.
[45] Gustafsson MV, Zheng X, Pereira T, Gradin K, Jin S, Lundkvist J, et al. Hypoxia requires notch signaling to maintain the undifferentiated cell state. Dev Cell 2005;9:617–28.
[46] Zhang D, Kilian KA. The effect of mesenchymal stem cell shape on the maintenance of multipotency. Biomaterials 2013;34:3962–9.
[47] Hsu SH, Ho TT, Huang NC, Yao CL, Peng LH, Dai NT. Substrate-dependent modulation of 3D spheroid morphology self-assembled in mesenchymal stem cell-endothelial progenitor cell coculture. Biomaterials 2014;35:7295–307.
[48] Song X, Zhu CH, Doan C, Xie T. Germline stem cells anchored by adherens junctions in the Drosophila ovary niches. Science 2002;296:1855–7.
[49] Garcion E, Halilagic A, Faissner A, ffrench-Constant C. Generation of an environmental niche for neural stem cell development by the extracellular matrix molecule tenascin C. Development 2004;131:3423–32.
[50] Keung AJ, Kumar S, Schaffer DV. Presentation counts: microenvironmental regulation of stem cells by biophysical and material cues. Annu Rev Cell Dev Biol 2010;26:533–56.
[51] Lee EJ, Park SJ, Kang SK, Kim GH, Kang HJ, Lee SW, et al. Spherical bullet formation via E-cadherin promotes therapeutic potency of mesenchymal stem cells derived from human umbilical cord blood for myocardial infarction. Mol Ther 2012;20:1424–33.
[52] Spencer HL, Eastham AM, Merry CL, Southgate TD, Perez-Campo F, Soncin F, et al. E-cadherin inhibits cell surface localization of the pro-migratory 5T4 oncofetal antigen in mouse embryonic stem cells. Mol Biol Cell 2007;18:2838–51.
[53] Li R, Liang J, Ni S, Zhou T, Qing X, Li H, et al. A mesenchymal-to-epithelial transition initiates and is required for the nuclear reprogramming of mouse fibroblasts. Cell Stem Cell 2010;7:51–63.
[54] Song X, Xie T. DE-cadherin-mediated cell adhesion is essential for maintaining somatic stem cells in the Drosophila ovary. Proc Natl Acad Sci U S A 2002;99:14813–8.
[55] Huang J, Chen T, Liu X, Jiang J, Li J, Li D, et al. More synergetic cooperation of Yamanaka factors in induced pluripotent stem cells than in embryonic stem cells. Cell Res 2009;19:1127–38.